nature communications

Article

https://doi.org/10.1038/s41467-023-43202-5

Mechanistic study on the side arm effect in a palladium/Xu-Phos-catalyzed enantioselective alkoxyalkenylation of γ-hydroxyalkenes

Received: 24 April 2023

Accepted: 3 November 2023

Published online: 22 November 2023

Check for updates

Shuai Zhu[1,5], Zihao Ye[2,5], Ming-Jie Chen[1,5], Lei Wang[3], Yu-Zhuo Wang[1], Ke-Nan Zhang[1], Wen-Bo Li[1], Han-Ming Ding[1], Zhiming Li[2] ✉ & Junliang Zhang[1,2,3,4] ✉

Recently, the asymmetric bifunctionalization of alkenes has received much attention. However, the development of enantioselective alkoxyalkenylation has posed a considerable challenge and has lagged largely behind. Herein, we report a new palladium-catalyzed enantioselective alkoxyalkenylation reaction, using a range of primary, secondary, and tertiary γ-hydroxy-alkenes with alkenyl halides. By employing newly identified Xu-Phos (**Xu8** and **Xu9**) with a suitable side-arm adjacent to the PCy_2 motif, a series of allyl-substituted tetrahydrofurans were obtained in good yields with up to 95% *ee*. Besides (*E*)-alkenyl halides, (*Z*)-alkenyl halide was also examined and provided the corresponding (*Z*)-product as a single diastereomer, supporting a stereospecific oxidative addition and reductive elimination step. Moreover, deuterium labeling and VCD experiments were employed to determine a *cis*-oxypalladation mechanism. DFT calculations helped us gain deeper insight into the side-arm effect on the chiral ligand. Finally, the practicability of this method is further demonstrated through a gram-scale synthesis and versatile transformations of the products.

Tetrahydrofuran derivatives bearing substituents at the C2 position are important subunits in pharmaceuticals, materials, and natural products (Fig. 1)[1–8]. Thus, many methods for stereoselective synthesis of multisubstituted tetrahydrofurans have been developed[9–24], among which metal-catalyzed cyclizations of readily available unsaturated alcohols have shown good performance in the synthesis of diverse tetrahydrofuran products with predictable regio- and diastereoselectivity[25–39]. The groups of Zurek, Chemler[40,41], and Liu[42] independently developed copper-catalyzed asymmetric radical alkene carboalkoxylation of γ-hydroxyalkenes, which provide facile access to chiral tetrahydrofurans with high enantioselectivities. Sigman and coworkers reported an efficient Pd/Cu co-catalyzed enantioselective alkene bifunctionalization reaction of γ-hydroxyalkenes via intramolecular oxypalladation and subsequent addition[43,44]. Using chiral salen-Co complexes, Kang achieved an elegant instance of enantioselective intramolecular iodoetherification to furnish such chiral five-membered oxygen heterocycles[45]. Regarding the significance of chiral tetrahydrofuran, the development of highly enantioselective

[1]Shanghai Key Laboratory of Green Chemistry and Chemical Processes, School of Chemistry and Molecular Engineering, East China Normal University, 3663 N. Zhongshan Road, Shanghai 200062, P.R. China. [2]Department of Chemistry, Fudan University, 2005 Songhu Road, Shanghai 200438, P.R. China. [3]School of Chemistry & Chemical Engineering, Yangzhou University, Yangzhou 225002, P.R. China. [4]School of Chemistry & Chemical Engineering, Henan Normal University, Xinxiang 453007 Henan, P.R. China. [5]These authors contributed equally: Shuai Zhu, Zihao Ye, Ming-Jie Chen. ✉e-mail: zmli@fudan.edu.cn; junliangzhang@fudan.edu.cn

methods for their synthesis from readily available starting materials, especially under mild conditions is still highly desirable.

Because alkenyl group can be converted into various functional groups, which is particularly important for increasing the diversity of compounds[46]. Several progresses have been achieved in alkenylation reactions, which provided efficient access to compounds with alkenyl framework. For instance, Sigman realized the aryl-alkenylation of unactivated alkenes with vinyl triflates and boronic acids furnishing skipped dienes, however, the substrates were limited to aryl 1,3-dienes[47]. Recently, Shu reported a cross-electrophile reaction of unactivated alkenes with vinyl triflates, which led to highly enantioselective aryl-alkenylation products including dihydrobenzofurans, indolines, and indanes in good yields with up to >99% *ee*[48]. Unfortunately, the related synthesis of enantiopure tetrahydrofurans with 2-allylic substituent from unactivated alkenols is rarely explored.

Wolfe and Tang's works have constructed a series of asymmetric oxygen-containing heterocyclic by Pd-catalyzed carboetherification reactions of alkenes with aryl bromides (Fig. 2a). However, the involvement of alkenyl bromides in the reaction has not been reported successfully, although Wolfe and Tang have made related attempts. The result indicates that the reactivity and enantioselectivity control of alkenyl bromine and aryl bromine in the reaction are very different, even though they are both C(sp^2)-Br in form. Inspired by the good performance of sulfinamide-phosphine (**Sadphos**) in asymmetric catalysis[49–58] and the unsuccess of the alkoxyalkenylation in Wolfe and Tang's previous work[59–61], we became very interested in the Pd-catalyzed asymmetric alkoxyalkenylation reaction of γ-hydroxy alkenes with alkenyl halides, which remains as an unsolved problem and pose considerable challenges: 1) the catalyst inhibition caused by competitive side reactions, including Heck reaction, β-hydride elimination and double bond migration of the γ-hydroxyalkene;[31,59–61] 2) whether metal-catalyzed terminal olefin nucleopalladation is *cis* or *trans*-attack has always been an open question[49,50]; 3) the asymmetric synthesis of tetrahydrofurans with a tertiary carbon center in one-step, especially under mild conditions[41,42]; 4) primary, secondary and tertiary γ-hydroxyalkenes provide products in good yield and *ee*[59–61].

Herein, we report new sulfinamide phosphine ligands (**Xu8** and **Xu9**) with a side-arm adjacent to the PCy_2 motif, which are crucial to address the challenging enantioselective alkoxyalkenylation reaction of γ-hydroxy-alkenes with alkenyl halides under mild conditions (Fig. 2b). Moreover, VCD method and DFT calculation are utilized to verify the *cis*-oxypalladation mechanism, which is usually ambiguous in similar reactions. Transition states for the *cis*-oxypalladation step are located and analyzed, revealing the origin of the side-arm effect in our ligands.

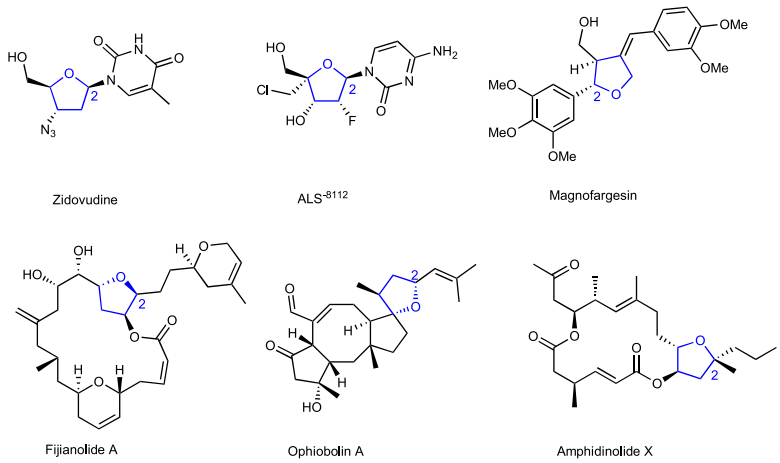

Fig. 1 | Biologically active compounds containing 2-substituted tetrahydrofuran skeletons. Substructures colored in blue highlight the core 2-substituted tetrahydrofuran skeleton with stereocenter. Zidovudine, an antimetabolite and a HIV-1 reverse transcriptase inhibitor. ALS^{-8112}, respiratory syncytial virus (RSV) polymerase inhibitor. Magnofargesin, a natural product found in *Magnolia biondii*. Fijianolide A, a natural compound isolated from *Spongia mycofijiensis*. Ophiobolin A, a fungal secondary metabolite has activity against glioblastoma. Amphidinolide X, a natural product isolated from *Amphidinium sp*.

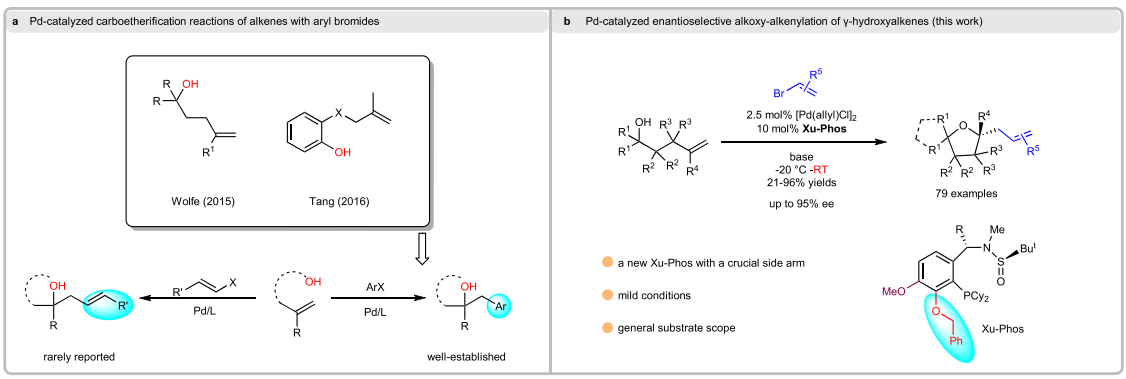

Fig. 2 | Background and reaction design. a Pd-catalyzed carboetherification reactions of alkenes with aryl bromides. **b** Pd-catalyzed enantioselective alkoxy-alkenylation of γ-hydroxyalkenes.

Results

Reaction Development

In our initial study, tertiary γ-hydroxyalkene **1a** and alkenyl bromide **2a** were selected as the model substrates. A series of privileged chiral ligands **L1-L8** were investigated, such as (*R*)-Tol-BINAP (**L1**), (*R*)-QuinoxP (**L2**), (*S*,*S*)-Me-duphos (**L3**), ferrocene ligands (**L4-L6**), (*S*,*S*)-DIOP (**L7**), (*R*)-BIDIME (**L8**), in which the (*R*)-BIDIME **L8** showed the promising result to deliver **3a** in 58% yield with 61% *ee* (Fig. 3). Next, we turned our attention to our developed sulfinamide-phosphine (**Sadphos**) ligand such as Xu-Phos (**Xu1**) with free N-H bond, unfortunately, it gives 33% yield and 2% *ee* (Fig. 3). To our delight, the N-Me-Xu-Phos (**Xu2**) could deliver the desired product in 81% yield with 85% *ee*. Then, we focused on adjusting the R group in the Xu-Phos (**Xu3, Xu4**), but no better results were obtained.

Inspired by Tang's findings that introducing a side-arm in the ligand is an efficient strategy to improve enantioselectivity by adjusting the electronic properties and space environment of the catalyst, like SaBOX ligands[62,63], we next designed and prepared new ligands **Xu5**-**Xu8**. These ligands bear a sterically congested substituent at the *ortho* position of the phosphine group (Fig. 3). The absolute configuration of **Xu6** was well established by X-ray crystallography analysis. Gratifyingly, ligand **Xu8**, easily prepared from 2-bromo-3-hydroxy-4-methoxybenz-aldehyde, delivers much better *ee* (92% *ee*) compared to **Xu6** (82% *ee*) under the conditions with the 2.5 mol% of $[Pd(allyl)Cl]_2$ and 10 mol% ligand, NaO^{t}Bu as the base, H_2O as the additive in Et_2O/hexane at RT. The introduction of a methoxy group into the *meta*-position of the phosphine group in ligand **Xu8** was critical to the stereoselectivity and reactivity. By changing *p*-Ph-C_6H_4 to 3,5-CF_3-C_6H_3, **Xu9** afforded the product in 63% yield with 90% *ee*. While changing OMe to OBn or OEt, **Xu10**, and **Xu12** gave comparative *ee* (89% *ee*, 90% *ee*) compared to **Xu8**. Furthermore, changing OMe to O^{i}Pr (**Xu13**), led to a lower ee (85% *ee*) compared to **Xu8**. Compared to **Xu3, Xu11**, which contained a methoxy group in the *para*- and *meta*-position of the ligand **Xu3**, yielded slightly lower results (52% yield, 84% *ee*). We proposed that the methoxy group substituent pushes the side-arm OBn much closer to the catalytic center, and steric effects between methoxy or other alkyloxy (OR) and OBn groups may be crucial for the high stereoselectivity of Xu-Phos.

To obtain better enantioselectivity (vide infra), further screening of the reaction conditions was examined. As shown in Table 1, the absence of H_2O resulted in **3a** with slightly inferior enantioselectivity (Table 1, entries 2–6). Investigation of palladium catalysts revealed that $[Pd(allyl)Cl]_2$ was most effective in this transformation (Table 1, entries 7–9). Changes of bases to KO^{t}Bu, LiO^{t}Bu, and Cs_2CO_3 led to a significant decrease in enantioselectivity (Table 1, entries 10–13). Using the NaOH instead of NaO^{t}Bu, can improve the enantioselectivity to 97% *ee*, but decrease the yield to 29% (Table 1, entry 13). And further solvent screening failed to improve the enantioselectivity (Table 1, entries 14–17).

Substrate scope of the reaction

With the optimal reaction conditions in hand (Table 1, entry 1), we evaluated the scope of alkenyl bromides (Fig. 4). The (*E*)-styrenyl bromide and phenyl substituents with electron-donating groups (Me, MeO) at *ortho*-, *meta*- and *para*-position worked well to form the corresponding compounds **3a-3e** in 51–74% yields with 90–92% *ee*s. Disubstituted and trisubstituted phenyl rings with OMe at different positions were also compatible, delivering the corresponding products **3f-3g** in 42–63% yields with 84–92% *ee*s. On the other hand, substrates with electron-withdrawing groups at *meta*- and

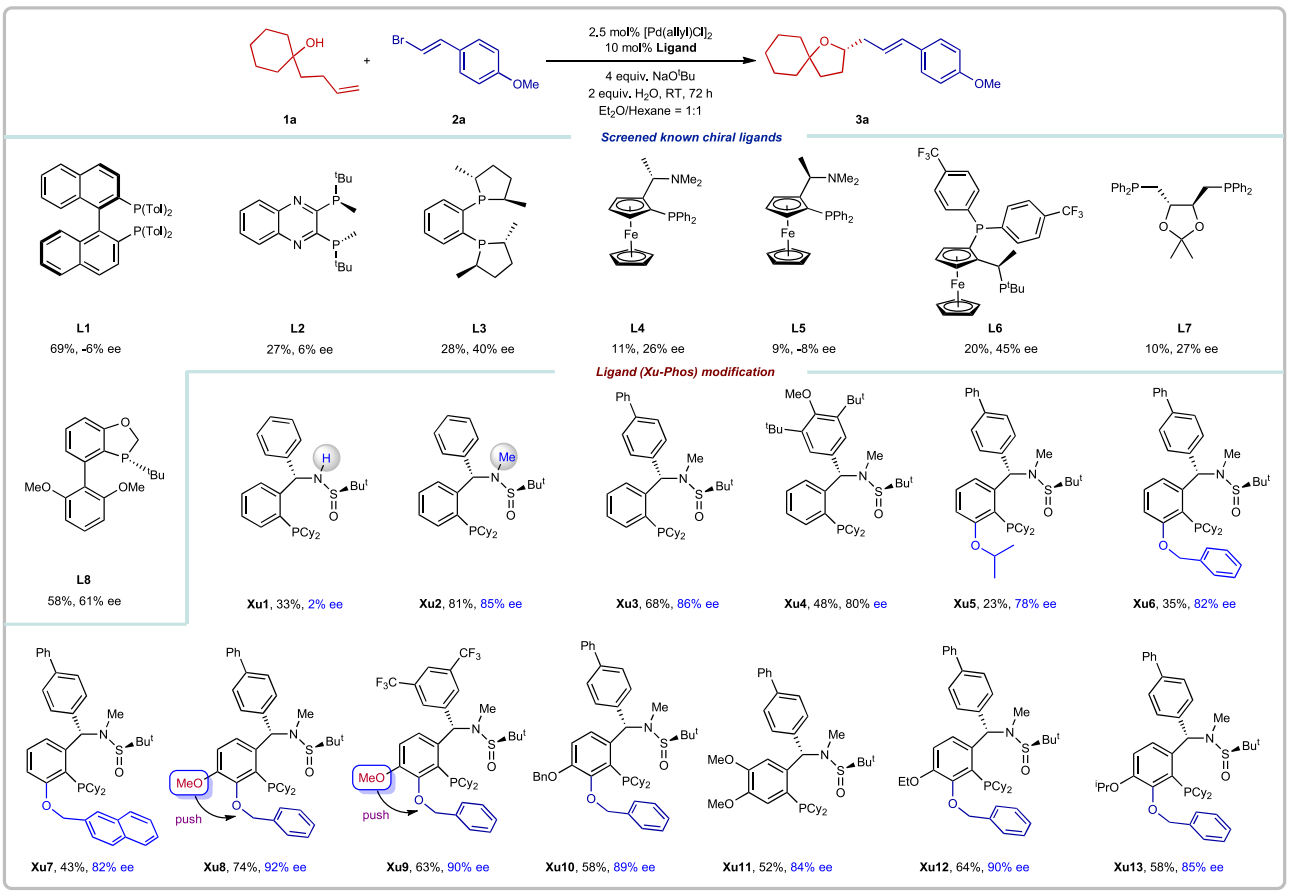

Fig. 3 | Screened chiral ligands. Reaction conditions: **1a** (0.1 mmol), **2a** (0.2 mmol), NaO^{t}Bu (4 equiv.), H_2O (2 equiv.), $[Pd(allyl)Cl]_2$ (2.5 mol%), **Xu8** (10 mol%) in 1 mL Et_2O/Hexane under N_2 at RT for 72 h. Isolated yields. *ee* was determined by chiral HPLC analysis.

https://doi.org/10.1038/s41467-023-43202-5

Table 1 | Optimization of the reaction conditions[a]

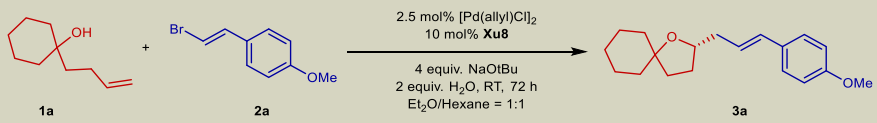

1a 2a 3a

Entry	Additive	[Pd]	Base	Solvent	Yield%	Ee%
1	H_2O	$[Pd(allyl)Cl]_2$	NaO^tBu	Et_2O/Hexane = 1:1	74	92
2	--	$[Pd(allyl)Cl]_2$	NaO^tBu	Et_2O/Hexane = 1:1	84	84
3	4 Å MS	$[Pd(allyl)Cl]_2$	NaO^tBu	Et_2O/Hexane = 1:1	79	91
4	MeOH	$[Pd(allyl)Cl]_2$	NaO^tBu	Et_2O/Hexane = 1:1	75	79
5	EtOH	$[Pd(allyl)Cl]_2$	NaO^tBu	Et_2O/Hexane = 1:1	54	70
6	^{i}PrOH	$[Pd(allyl)Cl]_2$	NaO^tBu	Et_2O/Hexane = 1:1	52	60
7	H_2O	$Pd(dba)_2$	NaO^tBu	Et_2O/Hexane = 1:1	43	93
8	H_2O	$Pd(OAc)_2$	NaO^tBu	Et_2O/Hexane = 1:1	72	92
9	H_2O	$PdCl_2$	NaO^tBu	Et_2O/Hexane = 1:1	12	78
10	H_2O	$[Pd(allyl)Cl]_2$	KO^tBu	Et_2O/Hexane = 1:1	–	–
11	H_2O	$[Pd(allyl)Cl]_2$	LiO^tBu	Et_2O/Hexane = 1:1	41	7
12	H_2O	$[Pd(allyl)Cl]_2$	Cs_2CO_3	Et_2O/Hexane = 1:1	15	85
13	H_2O	$[Pd(allyl)Cl]_2$	NaOH	Et_2O/Hexane = 1:1	29	97
14	H_2O	$[Pd(allyl)Cl]_2$	NaO^tBu	Toluene	90	91
15	H_2O	$[Pd(allyl)Cl]_2$	NaO^tBu	THF	51	90
16	H_2O	$[Pd(allyl)Cl]_2$	NaO^tBu	Et_2O	36	94
17	H_2O	$[Pd(allyl)Cl]_2$	NaO^tBu	Hexane	55	88

[a]Reaction conditions: **1a** (0.1 mmol), **2a** (0.2 mmol), NaO^tBu (4 equiv.), H_2O (2 equiv.), $[Pd(allyl)Cl]_2$ (2.5 mol%), **Xu8** (10 mol%) in 1 mL Et_2O/Hexane under N_2 at RT for 72 h. Isolated yields. *ee* was determined by chiral HPLC analysis.

https://doi.org/10.1038/s41467-023-43202-5

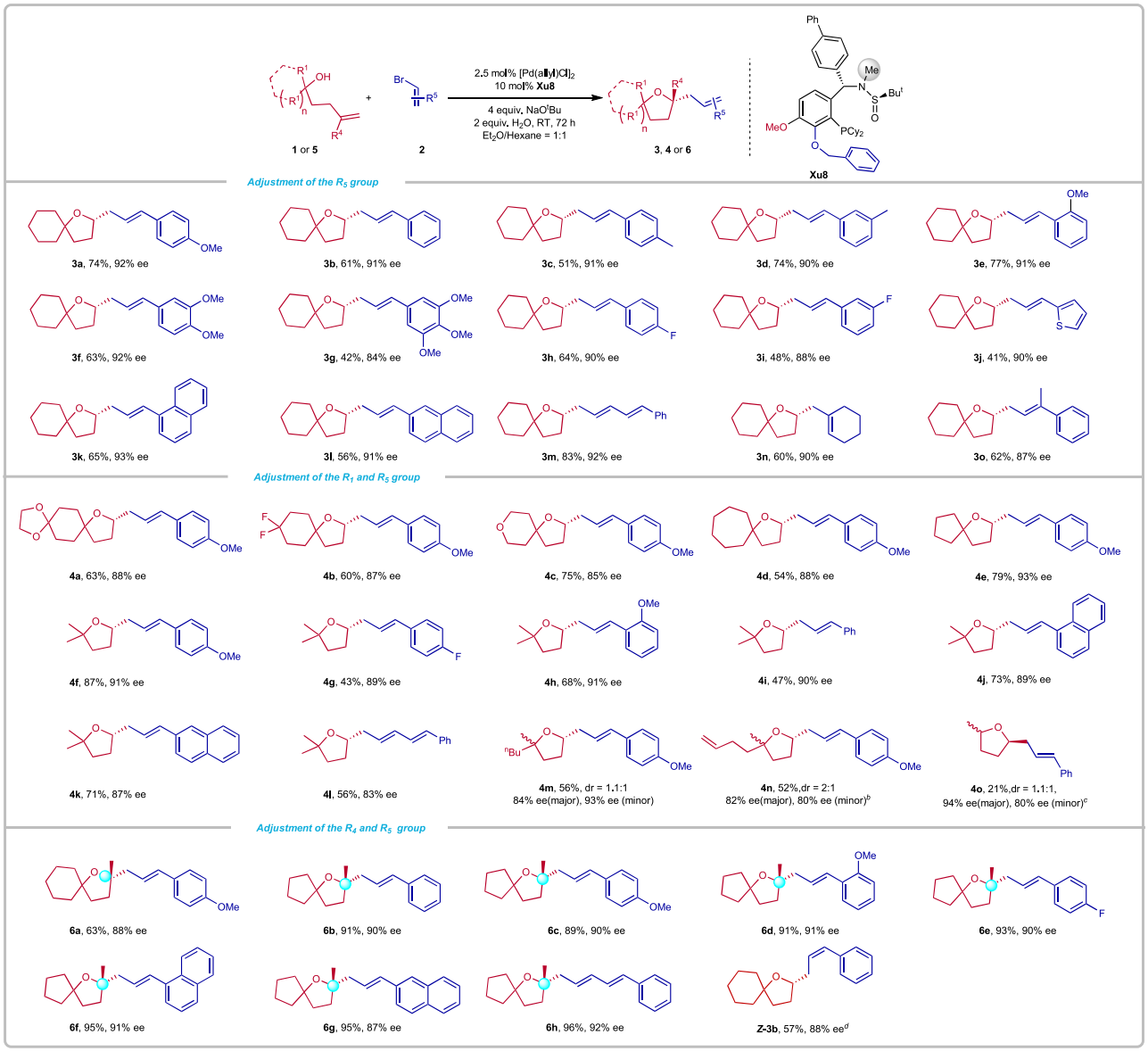

Fig. 4 | Synthesis of 3, 4, or 6. Reaction conditions: **1** or **5** (0.2 mmol), **2** (0.4 mmol), NaO^{t}Bu (4 equiv.), H_2O (2 equiv.), $[Pd(allyl)Cl]_2$ (2.5 mol%), **Xu8** (10 mol%) in 2 mL Et_2O/Hexane under N_2 at RT for 72 h. Isolated yields. *ee* was determined by chiral HPLC analysis. [b] with **Xu6** (10 mol%) in 2 mL toluene under N_2 at RT for 72 h. [c] 1 (0.5 mmol), 2 (1 mmol), EtONa (4 equiv.), $[Pd(allyl)Cl]_2$ (2.5 mol%), (*R*, R_S)-**Xu9** (10 mol%) in toluene under N_2 at −20 °C for 72 h. [d] 5 mol% $[Pd(allyl)Cl]_2$, 20 mol% **Xu2**.

para-position also proceeded well and generated **3h-3i** in 48–64% yields with 88–90% *ee*s. The phenyl group could be replaced by heteroaryl or other aryl groups, such as 2-thienyl, 2-naphthyl, and 1-naphthyl, delivering the desired **3j-3l** in 41–65% yields with 90–93% *ee*s. Furthermore, chain alkenyl bromide, cycloalkenyl bromide, and multi-substituted bromide were investigated, furnishing the relevant products **3 m, 3n**, and **3o** in 60–83% yields with 87–92% *ee*s. Next, we investigated different types of tertiary γ-hydroxyalkenes. We found that functionalized tertiary γ-hydroxyalkenes bearing the electron-donating (MeO) and electron-withdrawing (F) groups on the six-membered rings were well tolerated to afford the corresponding products **4a** and **4b** in 60–63% yields with 87–88% *ee*s. The pyran-derived tertiary γ-hydroxyalkene was also suitable for this transformation, delivering **4c** in 75% yield with 85% *ee*. Other cyclic γ-hydroxyalkenes containing seven- or five-membered rings were well compatible to furnish the corresponding products **4d** and **4e** in 54–79% yields with 88–93% *ee*s. The acyclic γ-hydroxyalkene has a good performance in this reaction, offering the alkoxyalkenylation products **4f-4l** in 43–87% yields with 83–91% *ee*s.

The cyclization of racemic γ-hydroxyalkene as the substrate furnished a 1.1:1 diastereomeric mixture of the product **4 m** in 56% yield with 84% and 93% *ee*. The desymmetrization of mesomeric γ-hydroxyalkene was realized by using **Xu6**, delivering **4n** in 52% yield as a 2:1 mixture of diastereomer with considerable *ee*. The secondary γ-hydroxyalkene also produced a mixture of diastereomers of **4o** in 21% yield with 94% *ee* and 80% *ee*. The relatively lower yield may be attributed to the competitive side oxidation reaction of the alcohol[59].

Further studies showed that a series of products bearing a tertiary stereocenter could be furnished in moderate to good yields with high enantioselectivities from the corresponding methyl-substituted tertiary γ-hydroxyalkenes (Fig. 4). Alkenes with a five- or six-membered ring were well tolerated to give the desired products **6a-6b** with 63–91% yields and 88–90% *ee*s. The reactions with a range of alkenyl bromides bearing a monosubstituted phenyl ring with an electron-donating group (OMe) or an electron-withdrawing group (F) at the *ortho*- or *para*-position furnished the desired products **6c-6e** in 89–93% yields with 90–91% *ee*s. The use of 1-naphthyl alkenyl bromides and 2-naphthyl alkenyl bromides delivered the enantiopure products

6f-6g bearing a quaternary stereocenter in 95% yields with 87–91% *ee*s. In addition, the 1,3-dienyl bromide was well compatible under the reaction condition, furnishing **6 h** in 96% yield with 92% *ee*.

It is well known that *Z*-olefins are the basic structural unit of organic molecules and thermodynamic unstable, rendering a jumbo challenge for the synthesis of functionalized *Z*-olefins with highly selectivity[64]. When the *Z*-alkenyl bromide **2b** was utilized in the reaction, the target product ***Z*-3b** could be obtained in 57% yield with 88% *ee* by using **Xu2** as the ligand (Fig. 4). This result indicated the alkene configuration was retained in this process.

After finished enantioselective alkoxyalkenylation reaction of tertiary γ-hydroxyalkenes, we turned to investigate the more challenging primary γ-hydroxy alkenes due to the competitive side reaction, i.e. the oxidation[59] (Fig. 5). Moreover, the enantiocontrol was believed to be more difficult than tertiary alcohols. Indeed, we didn't get good result (63% yield, 67% *ee*) at the beginning under standard conditions. Fortunately, another ligand **Xu9** was identified as a good ligand, delivering a very exciting result (68% yield, 92% *ee*) under the conditions with the 2.5 mol% of $[Pd(allyl)Cl]_2$ and 10 mol% ligand (**Xu9**), NaOEt as the base, in toluene at 0 °C. The scope of alkenyl bromides with primary γ-hydroxyalkenes was then investigated. A range of alkenyl bromides were compatible in the reaction. The alkenyl bromides bearing electron-donating groups on the R^2, such as alkyl group (**8c, 8d, 8e, 8 g**), alkyloxy (**8a, 8h-8k**), phenyl (**8 f**), and amino (**8 m**) coupled with **7** to afford products 44%-73% yields with high enantioselectivities (91–94% *ee*). However, the R^2 changing to 3,4,5-OMe-Ph (**8 l**), delivered a relatively lower yield, which might be due to the slow oxidation, but the enantioselectivity remains high (94% *ee*). Electron-withdrawing groups (**8n-8p**), thiophenyl (**8q**), and naphthyl (**8r, 8 s**) on the R^2 also could give satisfactory aim products. In these transformations, α-bromostyrene(**8 u**) and multi-substituted vinyl bromides(**8 v**) could also give good results.

Then, we turned our attention to investigating other primary γ-hydroxyalkenes bearing various substituents at different positions. The reaction with primary γ-hydroxyalkenes with substituted Bn groups at α-position proceeded smoothly to afford products **10a-10h** in moderate to good yields and high *ee*s. Besides Bn group, phenyl (**10j**), allyl (**10i**), and alkyl group (**10k-10n**) were also well tolerated, furnishing the products in 62–78% yields with 87–94% *ee*s. Next, we turned to examine the primary γ-hydroxyalkenes with two substituents at the β-position. The reaction temperature needed to be increased to 0 °C and the desired products **10o** and **10p** were obtained in 72% and

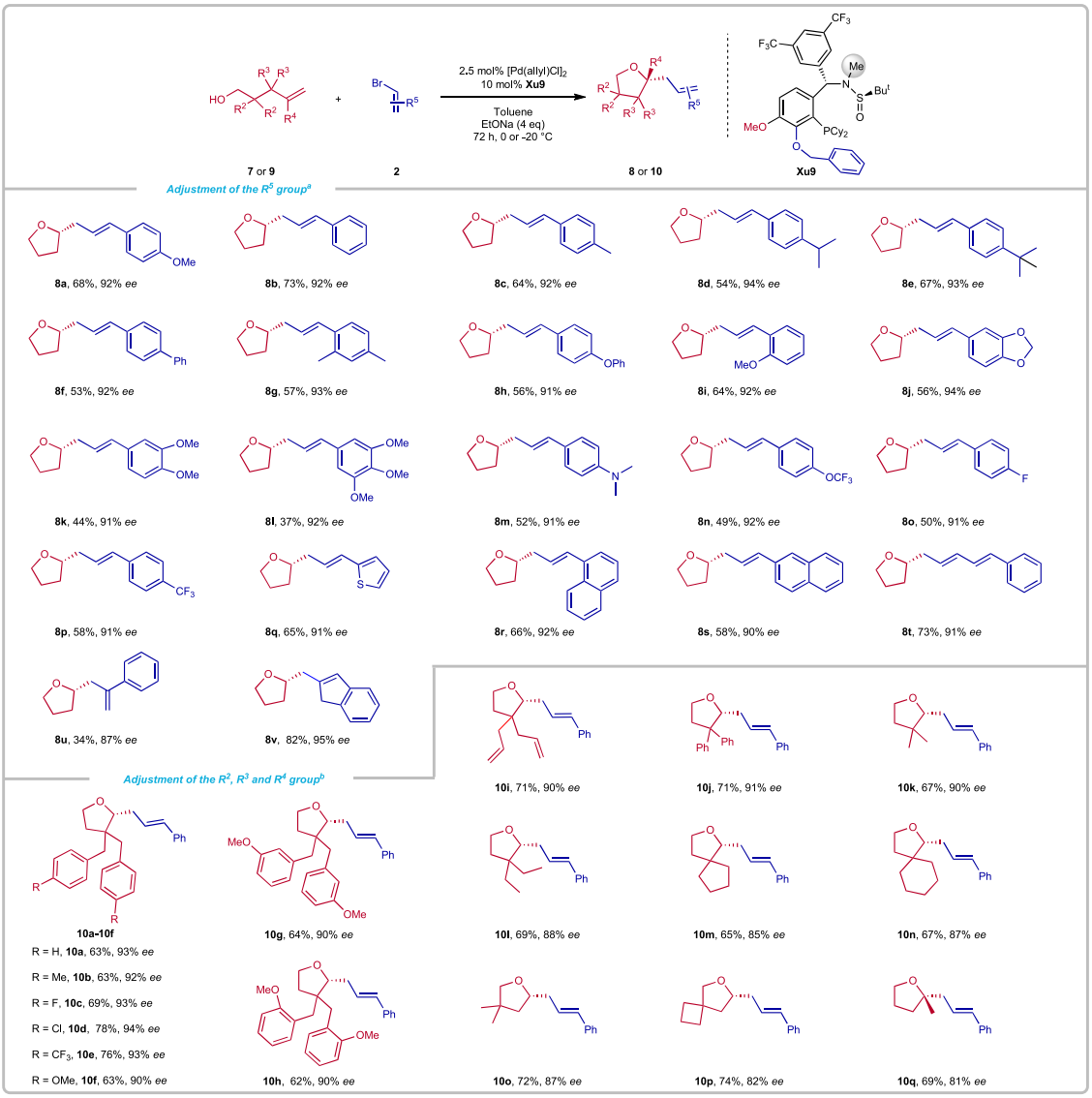

Fig. 5 | Synthesis of 8 or 10. Reaction conditions: **7** or **9** (0.5 mmol), **2** (1 mmol), EtONa (4 equiv.), $[Pd(allyl)Cl]_2$ (2.5 mol%), **Xu9** (10 mol%) in 3.5 mL toluene under N_2 for 72 h. Isolated yields. *ee* was determined by chiral HPLC analysis. [a]at 0 °C. [b]at −20 °C.

https://doi.org/10.1038/s41467-023-43202-5

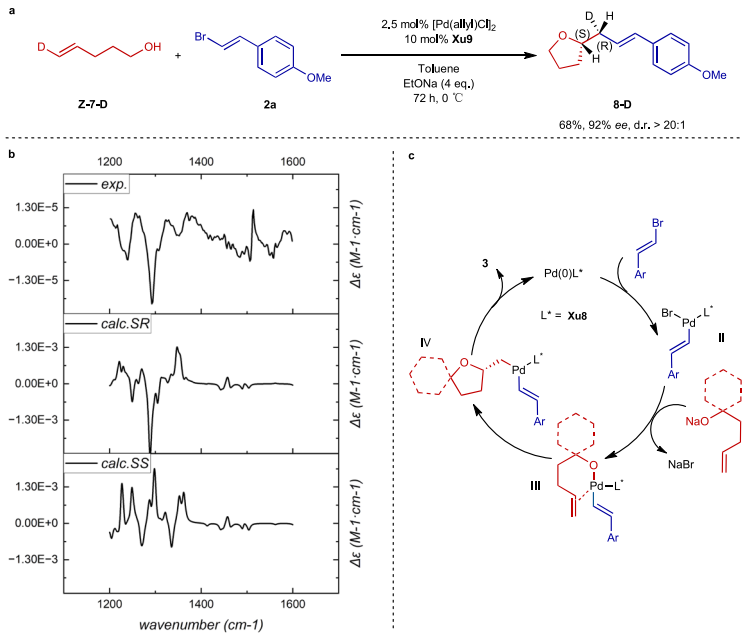

Fig. 6 | Investigation of the reaction mechanism. a Deuterium labeling experiment. **b** Comparison of experimental and computational VCD spectra. **c** Proposed catalytic cycle.

74% yield with 87% and 82% *ee*, respectively. Compound **10q** containing a tertiary stereocenter could also be obtained in 69% yield with 81% *ee* from the corresponding primary γ-hydroxyalkene with R^4 (methyl) group.

Mechanistic Investigation

To gain deep insight into the reaction mechanism and the origin of the stereoselectivity, further experimental and computational investigations were carried out. The *cis*- or *trans*-nucleopalladation attack of terminal alkenes has always been ambiguous since both patterns provide the same products. To determine the product's relative stereochemistry, we used the reaction of compound **7** labeled with deuterium (**Z-7-D**) and **2a** with **Xu9** as the ligand (Fig. 6a). The reaction achieved a high d.r. value (>20:1), indicating a highly specific mechanism of the oxypalladation step. Since the absolute configuration of the stereocenter in the THF ring was confirmed as *S* by XRD result (vide infra). We narrowed the possible stereochemistry of product **8** down to *SS* or *SR*. By comparing the experimental and computational (details provided in SI) VCD spectra (Fig. 6b), we found that **8-D** takes an *SR* configuration, which confirms a *cis*-oxypalladation operative mechanism. To the best of our knowledge, this is the first VCD application in the mechanism determination of organometallic reactions.

Based on the verified *cis*-oxypalladation mechanism, the proposed catalytic cycle is shown in Fig. 6c. First, the Pd^0 species is transformed into the Pd^{II} complex by the oxidative addition of alkenyl bromide (**2**). In the presence of NaO^{t}Bu and alcohol (**1**), the Pd–O bond is formed to afford complex **III** via ligand exchange. Then **III** proceeds a migratory insertion, delivering the Pd complex **IV**. This is the stereoselectivity-determining step. Through reductive elimination of complex **IV, 3** is obtained, and the catalyst can be regenerated. To further interrogate how our ligands may impart stereoselectivity, DFT calculations were performed. **Xu1, Xu2, Xu3, Xu6, Xu8, Xu9**, and corresponding substrates were taken as subjects. After thorough conformation searchs of the migratory insertion TSs (transition states), the calculated *ee* values match well with the experimental results (Supplementary Table 2). The TSs structures give us a way to inspect not only the origin of the high stereoselectivity, but also the unique role of the side-arm in enhancing the stereoselectivity.

Taking **Xu8** for example, three main factors may benefit the stereoselectivity. First, the conformation of the carbon chain of **1a** differs obviously between major and minor TSs. Intuitively, in the minor TS, **1a** interacts with the biphenyl substitution group of **Xu8** more intensively, causing the scaffold of the ligand to move correspondingly, resulting in some instability. Second, the conformational changes further affect the side-arm (OBn), and a significant conformational change of the side-arm is witnessed (Fig. 7a). In the major TS, a CH-π interaction is formed between the side-arm benzyloxy group and the vinyl substrate (shown as a green isosurface in Fig. 7a), which is absent in the minor TS. This stabilizes the major TS and benefits stereoselectivity (92% *ee*). Similar CH-π interaction and difference between major and minor TSs can be found in **Xu9** as well.

To disentangle possible controlling effects and provide quantitative proof for the analysis above, the energy difference ΔΔE between the major and minor TSs of **Xu6** and **Xu8** was decomposed. We compared the results of **Xu6** and **Xu8** and found that the energy difference between TSs mainly came from the dimer of Xu-Phos and vinyl substrate (Supplementary Table 4). Further decomposition of the energy indicated that the interaction between Xu-Phos and vinyl substrate is the main contributor (Fig. 7b). We investigated the strength of CH-π interactions between the side-arm benzyloxy group and vinyl substrate. Our computational analysis revealed an interaction energy of 3.6 kcal/mol (Fig. 7c)[65], which closely aligns with the Xu-Phos-vinyl substrate interaction energy difference between **Xu6** and **Xu8** (3.4 kcal/mol).

Furthermore, we observed that the substituent group *ortho* to the side-arm plays a crucial role in the side-arm effect. Specifically, in **Xu6**, the OBn group remained in the same position (resting position) in both TSs, and consequently had no impact on stereoselectivity (82% *ee*). However, when OMe was introduced in **Xu8**, the restricted space forced OBn to turn away from the resting position, leading to distinct conformations and, as a result, a more significant energy difference between the major and minor TSs. We conducted further theoretical and experimental analysis by substituting OMe with OEt, O^{i}Pr, and O^{t}Bu groups (Supplementary Table 6), which revealed that bulky groups (i.e. O^{i}Pr and O^{t}Bu) will interact with vinyl substrate instead of side-arm in minor TSs and reduced the energy difference between major and minor TSs. Consequently, it becomes evident that an

https://doi.org/10.1038/s41467-023-43202-5

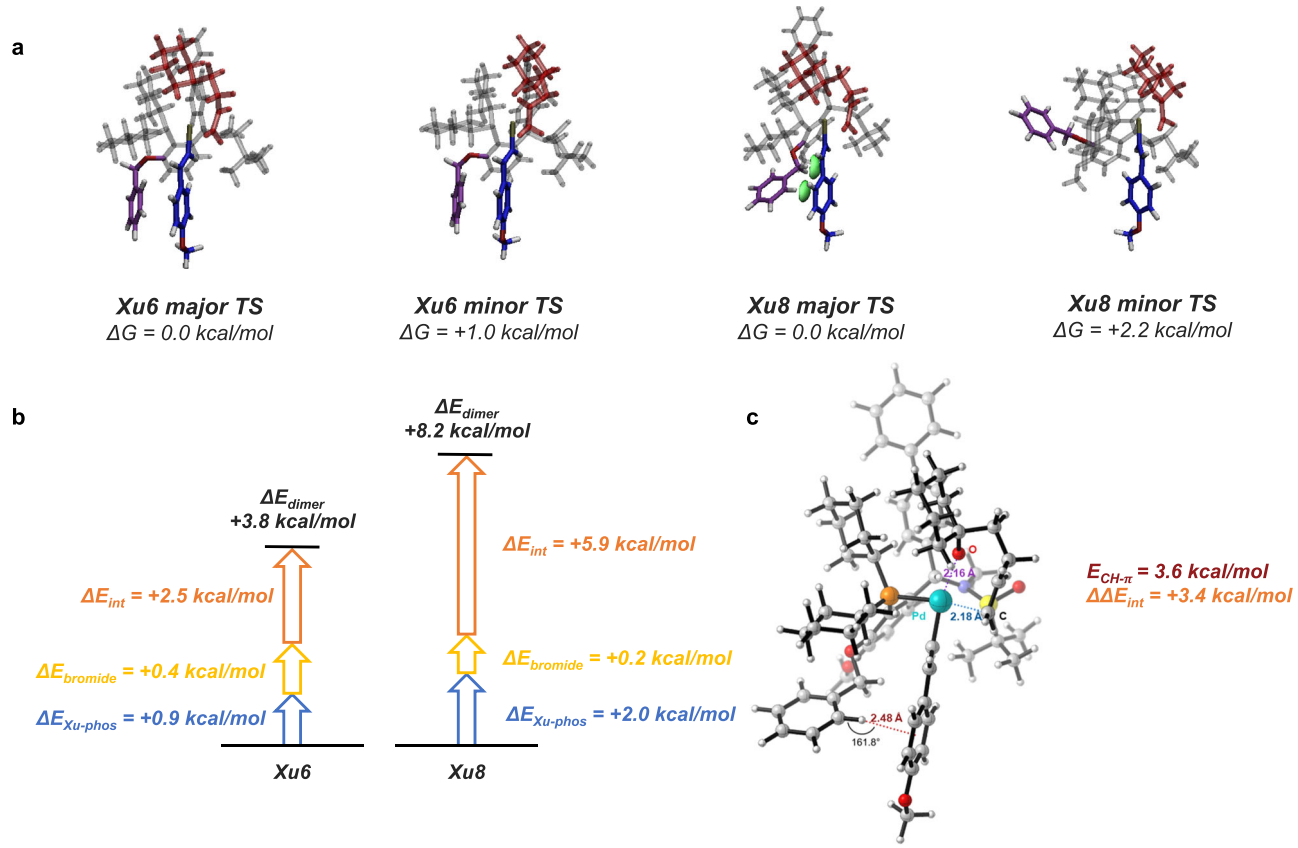

Fig. 7 | Visualization study and energy decomposition of the TSs. a Optimized TS structures for Pd/**Xu8** and Pd/Xu6 catalyzed reactions of 1a and 2a. CH-π interaction between side-arms and substrates in **Xu8** major is shown as green isosurfaces. **b** Energy difference decomposition result of Xu-Phos-vinyl substrate dimers. ΔE is calculated as minor structure energy subtracted major structure energy. $E_{Xu\text{-}Phos}$ represents the energy of Xu-Phos, E_{vinyl} represents the energy of the vinyl substrate, and E_{int} represents the interaction energy between Xu-Phos and the vinyl substrate. **c** The core structure and CH-π interaction of **Xu8** major TS. CH-π interaction is denoted with red dashed lines. The value of approximate intensity of the CH-π interaction and the difference of interaction energy between dimers in **Xu6** and **Xu8** are also shown.

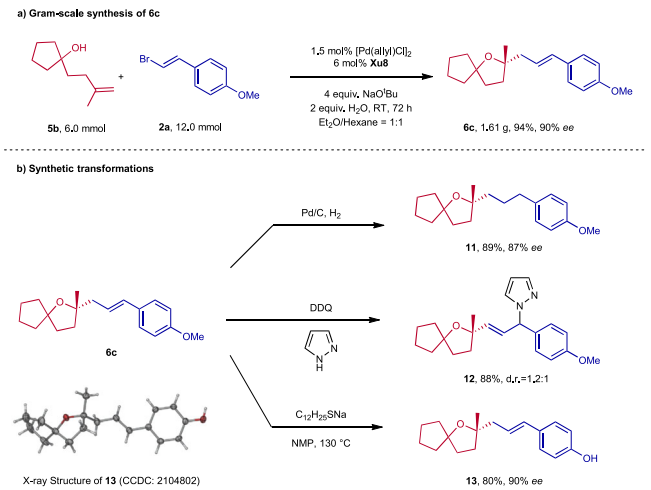

Fig. 8 | Gram-scale synthesis and transformations of products. a Gram-scale synthesis of 6c. **b** Synthetic transformations of 6c.

appropriate group situated adjacent to the side-arm must serve a dual purpose. Not only should it impart steric hindrance, but it should also strike a balance by avoiding excessive bulkiness that might trigger undesired interactions with the vinyl substrate.

To showcase the synthetic application of this methodology, a gram-scale reaction and several transformations of **6c** were carried out (Fig. 8). Under the catalysis of 1.5 mol% $[Pd(allyl)Cl]_2$ at RT, 1.61 g of **6c** was obtained in 94% yield with 90% *ee*. A hydrogenation reaction of **6c** delivered the corresponding product **11**. Treatment of **6c** with 1H-pyrazole under the oxidation of DDQ led to compound **12** with 1.2:1 dr. The enantiopure **6c** could undergo a demethylation reaction to produce compound **13**, whoseDiscussion.

In summary, we have developed an efficient palladium-catalyzed enantioselective alkoxyalkenylation of a range of primary, secondary, and tertiary γ-hydroxyalkenes with alkenyl halides. This reaction provides facile access to a series of enantiopure tetrahydrofurans containing an olefin framework with a tertiary or quaternary stereocenter. Notably, this process features a broad substrate scope, good functional group tolerance, and mild reaction conditions. Through a combination of experimental and DFT calculation investigation, we verified the *cis*-oxypalladium mechanism and located the stereo-determining TSs. Additionally, the introduction of a side-arm to the chiral ligand is a crucial strategy for achieving high efficiency and enantioselectivity. These findings offer exciting opportunities in asymmetric reactions, and the investigation of the side-arm effect may help in the rational design of chiral ligands.

Methods

General procedure for synthesis of 3, 4, or 6

To a sealed tube was added $[Pd(allyl)Cl]_2$ (2.5 mol%), **Xu8** (10 mol%). The flask was evacuated and refilled with argon. Then tertiary γ-hydroxyalkenes (0.2 mmol), alkenyl halides (0.4 mmol), NaO^{t}Bu (4.0 equiv.), H_2O (2.0 equiv.) and a mixed solution of Et_2O/Hexane (1: 1,

2 mL) was added to the tube and stirred at room temperature for 72 h. After the reaction was complete (monitored by TLC), the solvent was removed under reduced pressure. The crude product was then purified by flash column chromatography on silica gel to afford the desired product **3, 4**, or **6**.

General procedure for synthesis of 8 or 10

To a sealed tube was added $[Pd(allyl)Cl]_2$ (2.5 mol%), **Xu9** (10 mol%). The flask was evacuated and refilled with argon. Then γ-hydroxyalkenes (0.5 mmol), alkenyl halides (1 mmol), EtONa (4.0 equiv), and solution of toluene (3.5 mL) was added to the tube and stirred at 0 °C or -20 °C for 72 h. After the reaction was complete (monitored by TLC), the solvent was removed under reduced pressure. The crude product was then purified by flash column chromatography on silica gel to afford the desired product **8** or **10**.

Data availability

The data that support the findings of this study are available within the paper and its Supplementary Information files. The X-ray crystallographic coordinates for structures reported in this study have been deposited at the Cambridge Crystallographic Data Centre (CCDC), under deposition numbers 1977366 (**Xu6**-borane complex) and 2104802 (13). These data can be obtained free of charge from The Cambridge Crystallographic Data Centre via www.ccdc.cam.ac.uk/data_request/cif. The coordinates of DFT calculated structures are provided in Supplementary Information file. All data are also available from authors upon request.

References

1. Faul, M. M. & Huff, B. E. Strategy and Methodology Development for the Total Synthesis of Polyether Ionophore Antibiotics. *Chem. Rev.* **100**, 2407–2474 (2000).
2. Huo, J., Yang, S., Ding, J. & Yue, J. Cytotoxic Sesquiterpene Lactones from Eupatorium lindleyanum. *J. Nat. Prod.* **67**, 1470–1475 (2004).
3. Kang, E. J. & Lee, E. Total Synthesis of Oxacyclic Macrodiolide Natural Products. *Chem. Rev.* **105**, 4348–4378 (2005).
4. Miyazawa, M., Kasahara, H. & Kameoka, H. (-)-Magnofargesin and (+)-magnoliadiol, two lignans from Magnolia fargesii. *Phytochemistry* **42**, 531–533 (1996).
5. Noguchi, N. & Nakada, M. Synthetic Studies on (+)-Ophiobolin A: Asymmetric Synthesis of the Spirocyclic CD-Ring Moiety. *Org. Lett.* **8**, 2039–2042 (2006).
6. Lorente, A., Lamariano-Merketegi, J., Albericio, F. & Alvarez, M. Tetrahydrofuran-Containing Macrolides: A Fascinating Gift from the Deep Sea. *Chem. Rev.* **113**, 4567–4610 (2013).
7. Good, J. D., Mathews, N. & Cockerill, G. S. State of the Art in Respiratory Syncytial Virus Drug Discovery and Development. *J. Med. Chem.* **62**, 3206–3227 (2019).
8. Delost, M. D., Smith, D. T., Anderson, B. J. & Njardarson, J. T. From Oxiranes to Oligomers: Architectures of U.S. FDA Approved Pharmaceuticals Containing Oxygen Heterocycles. *J. Med. Chem.* **61**, 10996–11020 (2018).
9. Wolfe, J. P. Palladium-Catalyzed Carboetherification and Carboamination Reactions of γ-Hydroxy- and γ-Aminoalkenes for the Synthesis of Tetrahydrofurans and Pyrrolidines. *Eur. J. Org. Chem.* **2007**, 571–582 (2007).
10. Wolfe, J. P. & Hay, M. B. Recent advances in the stereoselective synthesis of tetrahydrofurans. *Tetrahedron* **63**, 261–290 (2007).
11. Jalce, G., Franck, X. & Figadère, B. Diastereoselective synthesis of 2,5-disubstituted tetrahydrofurans. *Tetrahedron: Asymmetry* **20**, 2537–2581 (2009).
12. Majumdar, K. C., Debnath, P. & Roy, B. Metal-Catalyzed Heterocyclization: Formation of Five- and Six-Membered Oxygen Heterocycles through Carbon-Oxygen Bond Forming Reactions. *Heterocycles* **78**, 2661–2728 (2009).
13. Chen, G. & Ma, S. Enantioselective Halocyclization Reactions for the Synthesis of Chiral Cyclic Compounds. *Angew. Chem. Int. Ed.* **49**, 8306–8308 (2010).
14. Zafrani, Y. et al. CF_2H, a Functional Group-Dependent Hydrogen-Bond Donor: Is It a More or Less Lipophilic Bioisostere of OH, SH, and CH_3? *J. Med. Chem.* **62**, 5628–5637 (2019).
15. Wolfe, J. P. Stereoselective Synthesis of Saturated Heterocycles via Palladium-Catalyzed Alkene Carboetherification and Carboamination Reactions. *Synlett* **19**, 2913–2937 (2008).
16. Wolfe, J. P. Synthesis of Saturated Heterocycles via Metal-Catalyzed Alkene Carboamination or Carboalkoxylation Reactions. *Top. Heterocycl. Chem.* **32**, 1–37 (2013).
17. Garlets, Z. J., White, D. R. & Wolfe, J. P. Recent Developments in Pd^0-Catalyzed Alkene-Carboheterofunctionalization Reactions. *Asian J. Org. Chem.* **6**, 636–653 (2017).
18. Kuwano, R. Catalytic Asymmetric Hydrogenation of 5-Membered Heteroaromatics. *Heterocycles* **76**, 909–922 (2008).
19. Tietze, L. F., Sommer, K. M., Zinngrebe, J. & Stecker, F. Palladium-Catalyzed Enantioselective Domino Reaction for the Efficient Synthesis of Vitamin E. *Angew. Chem. Int. Ed.* **44**, 257–259 (2005).
20. Jiao, Z. et al. Organocatalytic Asymmetric Direct Csp3-H Functionalization of Ethers: A Highly Efficient Approach to Chiral Spiroethers. *Angew. Chem. Int. Ed.* **51**, 8811–8815 (2012).
21. Zi, W. & Toste, F. D. Gold(I)-Catalyzed Enantioselective Desymmetrization of 1,3-Diols through Intramolecular Hydroalkoxylation of Allenes. *Angew. Chem. Int. Ed.* **54**, 14447–14451 (2015).
22. Rexit, A. A. & Mailikezati, M. Asymmetric synthesis of optically active spiroacetals from alkynyl glycols catalyzed by gold complex/Brønsted acid binary system. *Tetrahedron Lett.* **56**, 2651–2655 (2015).
23. Yu, S., Wu, C. & Ge, S. Cobalt-Catalyzed Asymmetric Hydroboration/Cyclization of 1,6-Enynes with Pinacolborane. *J. Am. Chem. Soc.* **139**, 6526–6529 (2017).
24. Wang, G. et al. Catalytic enantioselective oxidative coupling of saturated ethers with carboxylic acid derivatives. *Nat. Commun.* **10**, 559–567 (2019).
25. Zhang, G., Cui, L., Wang, Y. & Zhang, L. Homogeneous Gold-Catalyzed Oxidative Carboheterofunctionalization of Alkenes. *J. Am. Chem. Soc.* **132**, 1474–1475 (2010).
26. White, D. R. & Wolfe, J. P. Stereocontrolled Synthesis of Amino-Substituted Carbocycles by Pd-Catalyzed Alkene Carboamination Reactions. *Chem. Eur. J.* **23**, 5419–5423 (2017).
27. Ward, A. F. & Wolfe, J. P. Highly Diastereoselective Pd-Catalyzed Carboetherification Reactions of Acyclic Internal Alkenes. Stereoselective Synthesis of Polysubstituted Tetrahydrofurans. *Org. Lett.* **12**, 1268–1271 (2010).
28. Protti, S., Dondi, D., Fagnoni, M. & Albini, A. Photochemical Arylation of Alkenols: Role of Intermediates and Synthetic Significance. *Eur. J. Org. Chem.* **2008**, 2240–2247 (2008).
29. Nicolai, S. & Waser, J. Pd(0)-Catalyzed Oxy- and Aminoalkynylation of Olefins for the Synthesis of Tetrahydrofurans and Pyrrolidines. *Org. Lett.* **13**, 6324–6327 (2011).
30. Nicolai, S., Erard, S., González, D. F. & Waser, J. Pd-Catalyzed Intramolecular Oxyalkynylation of Alkenes with Hypervalent Iodine. *Org. Lett.* **12**, 384–387 (2010).
31. Hay, M. B. & Wolfe, J. P. Palladium-Catalyzed Synthesis of 2,1′-Disubstituted Tetrahydrofurans from γ-Hydroxy Internal Alkenes. Evidence for Alkene Insertion into a Pd–O Bond and Stereochemical Scrambling via β-Hydride Elimination. *J. Am. Chem. Soc.* **127**, 16468–16476 (2005).
32. Hay, M. B., Hardin, A. R. & Wolfe, J. P. Palladium-Catalyzed Synthesis of Tetrahydrofurans from γ-Hydroxy Terminal Alkenes: Scope,

Limitations, and Stereoselectivity. *J. Org. Chem.* **70**, 3099–3107 (2005).
33. Fries, P., Halter, D., Kleinschek, A. & Hartung, J. Functionalized Tetrahydrofurans from Alkenols and Olefins/Alkynes via Aerobic Oxidation–Radical Addition Cascades. *J. Am. Chem. Soc.* **133**, 3906–3912 (2011).
34. Zhu, C. & Falck, J. R. Alternative Pathways for Heck Intermediates: Palladium-Catalyzed Oxyarylation of Homoallylic Alcohols. *Angew. Chem. Int. Ed.* **50**, 6626–6629 (2011).
35. Schuch, D., Fries, P., Dönges, M., Pérez, B. M. & Hartung, J. Reductive and Brominative Termination of Alkenol Cyclization in Aerobic Cobalt-Catalyzed Reactions. *J. Am. Chem. Soc.* **131**, 12918–12920 (2009).
36. Palmer, C. et al. Increased Yields and Simplified Purification with a Second-Generation Cobalt Catalyst for the Oxidative Formation of trans-THF Rings. *Org. Lett.* **11**, 5614–5617 (2009).
37. Ball, L. T., Green, M., Lloyd-Jones, G. C. & Russell, C. A. Arylsilanes: Application to Gold-Catalyzed Oxyarylation of Alkenes. *Org. Lett.* **12**, 4724–4727 (2010).
38. McDonald, R. I., Liu, G. & Stahl, S. S. Palladium(II)-Catalyzed Alkene Functionalization via Nucleopalladation: Stereochemical Pathways and Enantioselective Catalytic Applications. *Chem. Rev.* **111**, 2981–3019 (2011).
39. Dohanosova, J. & Gracza, T. Asymmetric Palladium-Catalysed Intramolecular Wacker-Type Cyclisations of Unsaturated Alcohols and Amino Alcohols. *Molecules* **18**, 6173–6192 (2013).
40. Bovino, M. T. et al. Enantioselective Copper-Catalyzed Carboetherification of Unactivated Alkenes. *Angew. Chem. Int. Ed.* **53**, 6383–6387 (2014).
41. Karyakarte, S. D., Um, C., Berhane, I. A. & Chemler, S. R. Synthesis of Spirocyclic Ethers by Enantioselective Copper-Catalyzed Carboetherification of Alkenols. *Angew. Chem. Int. Ed.* **57**, 12921–12924 (2018).
42. Cheng, Y., Dong, X., Gu, Q., Yu, Z. & Liu, X. Achiral Pyridine Ligand-Enabled Enantioselective Radical Oxytrifluoromethylation of Alkenes with Alcohols. *Angew. Chem. Int. Ed.* **56**, 8883–8886 (2017).
43. Pathak, T. P., Gligorich, K. M., Welm, B. E. & Sigman, M. S. Synthesis and Preliminary Biological Studies of 3-Substituted Indoles Accessed by a Palladium-Catalyzed Enantioselective Alkene Difunctionalization Reaction. *J. Am. Chem. Soc.* **132**, 7870–7871 (2010).
44. Jensen, K. H., Webb, J. D. & Sigman, M. S. Advancing the Mechanistic Understanding of an Enantioselective Palladium-Catalyzed Alkene Difunctionalization Reaction. *J. Am. Chem. Soc.* **132**, 17471–17482 (2010).
45. Lee, S. B., Park, C. M. & Kang, S. H. Catalytic Enantioselective Iodocyclization of γ-Hydroxy-cis-alkenes. *J. Am. Chem. Soc.* **125**, 15748–15749 (2003).
46. McCammant, M. S., Liao, L. & Sigman, M. S. Palladium-Catalyzed 1,4-Difunctionalization of Butadiene To Form Skipped Polyenes. *J. Am. Chem. Soc.* **135**, 4167–4170 (2013).
47. Liao, L., Jana, R., Urkalan, K. B. & Sigman, M. S. A Palladium-Catalyzed Three-Component Cross-Coupling of Conjugated Dienes or Terminal Alkenes with Vinyl Triflates and Boronic Acids. *J. Am. Chem. Soc.* **133**, 5784–5787 (2011).
48. Tian, Z. et al. Highly Enantioselective Cross-Electrophile Aryl-Alkenylation of Unactivated Alkenes. *J. Am. Chem. Soc.* **141**, 7637–7643 (2019).
49. Zhang, Z. et al. Palladium/XuPhos-Catalyzed Enantioselective Carboiodination of Olefin-Tethered Aryl Iodides. *J. Am. Chem. Soc.* **141**, 8110–8115 (2019).
50. Zhang, Z. et al. Palladium-Catalyzed Enantioselective Reductive Heck Reactions: Convenient Access to 3,3-Disubstituted 2,3-Dihydrobenzofuran. *Angew. Chem. Int. Ed.* **57**, 10373–10377 (2018).
51. Zhou, W. et al. Chiral Sulfinamide Bisphosphine Catalysts: Design, Synthesis, and Application in Highly Enantioselective Intermolecular Cross-Rauhut–Currier Reactions. *Angew. Chem. Int. Ed.* **54**, 14853–14857 (2015).
52. Zhang, Z., Xu, B., Xu, S., Wu, H. & Zhang, J. Diastereo- and Enantioselective Copper(I)-Catalyzed Intermolecular [3+2] Cycloaddition of Azomethine Ylides with β-Trifluoromethyl β, β-Disubstituted Enones. *Angew. Chem. Int. Ed.* **55**, 6324–6328 (2016).
53. Zhang, Z. et al. A New Type of Chiral Sulfinamide Monophosphine Ligands: Stereodivergent Synthesis and Application in Enantioselective Gold(I)-Catalyzed Cycloaddition Reactions. *Angew. Chem. Int. Ed.* **53**, 4350–4354 (2014).
54. Zhang, P., Wang, Y., Zhang, Z. & Zhang, J. Gold(I)/Xiang-Phos-Catalyzed Asymmetric Intramolecular Cyclopropanation of Indenes and Trisubstituted Alkenes. *Org. Lett.* **20**, 7049–7052 (2018).
55. Wang, Y. et al. Gold-Catalyzed Asymmetric Intramolecular Cyclization of N-Allenamides for the Synthesis of Chiral Tetrahydrocarbolines. *Angew. Chem. Int. Ed.* **56**, 15905–15909 (2017).
56. Wang, L. et al. Enantioselective Synthesis of Isoxazolines Enabled by Palladium-Catalyzed Carboetherification of Alkenyl Oximes. *Angew. Chem. Int. Ed.* **59**, 4421–4427 (2020).
57. Wang, L., Chen, M., Zhang, P., Li, W. & Zhang, J. Palladium/PC-Phos-Catalyzed Enantioselective Arylation of General Sulfenate Anions: Scope and Synthetic Applications. *J. Am. Chem. Soc.* **140**, 3467–3473 (2018).
58. Hu, H. et al. Enantioselective gold-catalyzed intermolecular [2 + 2]-cycloadditions of 3-styrylindoles with N-allenyl oxazolidinone. *Org. Chem. Front.* **3**, 759–763 (2016).
59. Wolfe, J. P. & Ross, M. A. Stereoselective Synthesis of Tetrahydrofurans via the Palladium-Catalyzed Reaction of Aryl Bromides with γ-Hydroxy Alkenes: Evidence for an Unusual Intramolecular Olefin Insertion into a Pd(Ar)(OR) Intermediate. *J. Am. Chem. Soc.* **126**, 1620–1621 (2004).
60. Hopkins, B. A., Garlets, Z. J. & Wolfe, J. P. Development of Enantioselective Palladium-Catalyzed Alkene Carboalkoxylation Reactions for the Synthesis of Tetrahydrofurans. *Angew. Chem. Int. Ed* **54**, 13390–13392 (2015).
61. Hu, N., Li, K., Wang, Z. & Tang, W. Synthesis of Chiral 1,4-Benzodioxanes and Chromans by Enantioselective Palladium-Catalyzed Alkene Aryloxyarylation Reactions. *Angew. Chem. Int. Ed.* **55**, 5044–5048 (2016).
62. Liao, S., Sun, X. & Tang, Y. Side Arm Strategy for Catalyst Design: Modifying Bisoxazolines for Remote Control of Enantioselection and Related. *Acc. Chem. Res.* **47**, 2260–2272 (2014).
63. Wang, L., Zhou, J. & Tang, Y. Sidearm Modified Bisoxazo line Ligands and Their Applications. *Chin. J. Chem.* **36**, 1123–1129 (2018).
64. Siau, W., Zhang, Y. & Zhao, Y. in Stereoselective Alkene Synthesis, (Springer, Berlin, ed. 327, 2012), pp. 33–58.
65. Seguin, T. J., Lu, T. & Wheeler, S. E. Enantioselectivity in Catalytic Asymmetric Fischer Indolizations Hinges on the Competition of π-Stacking and CH/π Interactions. *Org. Lett.* **17**, 3066–3069 (2015).

Acknowledgements

We gratefully acknowledge the funding support of NSFC (22031004 and 21921003 for J.Z., and 22071060 for W.L.), National Key R&D Program of China (2021YFF0701600 for J.Z.) Shanghai Municipal Education Commission (20212308 for J.Z.), and Shanghai Science and Technology Commission (23ZR1404800 for Z.L.).

Author contributions

J.Z. conceived the project. J.Z., Z.L., S.Z., M.C., Z.Y. and W.L. wrote the paper. S.Z. and M.C. performed the experiments and analyzed the data. Z.Y. and Z.L. conducted the computational studies. L.W., Z.W., K.Z., and H.D. analyzed the data. All authors discussed the results and commented on the paper.

Competing interests
The authors declare no competing interests.

Additional information
Supplementary information The online version contains supplementary material available at https://doi.org/10.1038/s41467-023-43202-5.

Correspondence and requests for materials should be addressed to Zhiming Li or Junliang Zhang.

Peer review information *Nature Communications* thanks Paul Nicu, and the other, anonymous, reviewers for their contribution to the peer review of this work. A peer review file is available.

Reprints and permissions information is available at http://www.nature.com/reprints

Publisher's note Springer Nature remains neutral with regard to jurisdictional claims in published maps and institutional affiliations.

Open Access This article is licensed under a Creative Commons Attribution 4.0 International License, which permits use, sharing, adaptation, distribution and reproduction in any medium or format, as long as you give appropriate credit to the original author(s) and the source, provide a link to the Creative Commons licence, and indicate if changes were made. The images or other third party material in this article are included in the article's Creative Commons licence, unless indicated otherwise in a credit line to the material. If material is not included in the article's Creative Commons licence and your intended use is not permitted by statutory regulation or exceeds the permitted use, you will need to obtain permission directly from the copyright holder. To view a copy of this licence, visit http://creativecommons.org/licenses/by/4.0/.

© The Author(s) 2023